

Communication

# Reactive Polymorphic Nanoparticles: Preparation *via* Polymerization-induced Self-assembly and Post-synthesis Thiol-*para*-Fluoro Core Modification

Nicolas Busatto, Vlad Stolojan, Michael Shaw, Joseph L. Keddie, Peter J. Roth\*

---

Nicolas Busatto, Dr Peter J. Roth  
Department of Chemistry  
University of Surrey, Guildford, Surrey, GU2 7XH, UK  
\*E-mail: p.roth@surrey.ac.uk

Dr Vlad Stolojan  
Advanced Technology Institute  
University of Surrey, Guildford, Surrey, GU2 7XH, UK

Prof Joseph L. Keddie  
Department of Physics  
University of Surrey, Guildford, Surrey, GU2 7XH, UK

Dr Michael Shaw  
National Physical Laboratory,  
Hampton Road, Teddington, Middlesex, TW11 0LW, UK

Dr Michael Shaw  
Department of Computer Science  
University College London, London, WC1 6BT, UK

---

## Abstract

The use of 2,3,4,5,6-pentafluorobenzyl methacrylate (PFBMA) as a core-forming monomer in ethanolic RAFT dispersion polymerization formulations is presented. Poly[poly(ethylene glycol) methyl ether methacrylate] (pPEGMA) macromolecular chain transfer agents were chain extended with PFBMA leading to nanoparticle formation via polymerization-induced self-assembly (PISA). pPEGMA-pPFBMA particles exhibited the full range of morphologies (spheres, worms, and vesicles) including pure and mixed phases. Worm phases formed gels that underwent a thermo-reversible degelation and morphological transition to spheres (or spheres and vesicles) upon heating. Post-synthesis, the pPFBMA cores were modified through thiol-*para*-fluoro substitution reactions in ethanol using 1,8-diazabicyclo[5.4.0]undec-7-ene (DBU) as the base. For monothiols, conversions were 64% (1-octanethiol) and 94% (benzyl mercaptan). Spherical and worm-shaped nano-objects were core cross-linked using 1,8-octanedithiol, which prevented their dissociation in non-selective solvents. For a temperature-responsive worm sample, cross-linking additionally resulted in the loss of the temperature-triggered morphological transition. The use of the reactive monomer PFBMA in PISA formulations presents a simple method to prepare well-defined nano-objects similar to those produced with non-reactive monomers (*e.g.* benzyl methacrylate) and to retain morphologies independent of solvent and temperature.

## 1. Introduction

Polymerization-induced self-assembly (PISA) has been extensively used in recent years to prepare nanoparticles of well-defined morphologies. The method is based on the chain extension of a solubilising block with a second monomer in a selective solvent, leading to phase separation and the formation of nano-assemblies. Continuing growth of the core-forming block can cause the nano-objects to transition from spherical (S) to worm-like (W) and vesicular (V) morphology, enabling the preparation of these distinctly shaped soft matter particles.<sup>[1-6]</sup> Additionally, stimulus-responsive PISA particles can undergo morphological order–order transitions post-synthesis in response to temperature or pH triggers.<sup>[3, 4, 7]</sup> More recently, there has been increased interest in reactive PISA particles in order to introduce further chemical functionality,<sup>[8-10]</sup> or to evoke morphological transitions, for example to release encapsulated cargo.<sup>[11, 12]</sup> Such chemical manipulation is commonly performed on the solubilising block. Requirements for the core-forming species (monomer solubility, polymer insolubility, stability and compatibility during radical polymerization), on the other hand, limit the number of “second” monomers suitable for successful formulations. For PISA conducted in alcoholic dispersion, styrene, benzyl methacrylate, and phenylalkyl methacrylate homologues have been the most commonly employed core-forming monomers.<sup>[4]</sup> Chemical cross-linking of the core-forming blocks has been reported using diamines on ketone-functional monomers<sup>[13-15]</sup> and 3-aminopropyltriethoxysilane to react with PISA cores containing epoxides and hydroxyl groups<sup>[16]</sup>.

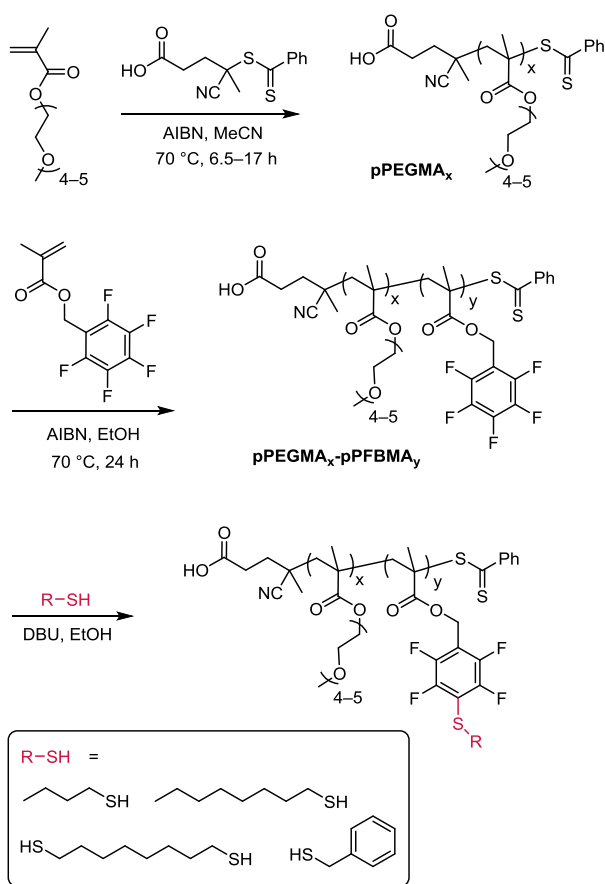
Recently,<sup>[17]</sup> Noy et al. demonstrated that poly(2,3,4,5,6-pentafluorobenzyl methacrylate) (pPFBMA) is a versatile reactive precursor that undergoes efficient nucleophilic aromatic *para*-fluoro substitution reactions with amines, thiols, and carbonylthiolates.<sup>[18, 19]</sup> Hence, it offers an attractive platform for follow-on chemical functionalization. Previously, Pei et al.

exploited Passerini multicomponent reaction-prepared pentafluorobenzyl-functional monomers for the post-synthesis surface functionalization of PISA-made nanoparticles.<sup>[8]</sup>

Herein, 2,3,4,5,6-pentafluorobenzyl methacrylate (PFBMA) is used for the first time as a core-forming monomer in alcoholic PISA formulations and shown to fulfil the above requirements. Thus, spherical, worm-shaped, and vesicular particles were obtained, including worm samples that underwent thermoreversible morphology transitions. The pentafluorobenzyl groups were stable during polymerization and allowed for efficient post-synthesis modification with thiols, which is exploited herein for cross-linking.

## **2. Results and discussion**

Reactive PISA particles of different morphologies were prepared by reversible addition-fragmentation chain transfer (RAFT) dispersion polymerization of pentafluorobenzyl methacrylate (PFBMA), mediated by poly[poly(ethylene glycol) methyl ether methacrylate] (pPEGMA) macromolecular chain transfer agents (macro-CTAs) in ethanol. Post-polymerization, the resulting pPEGMA<sub>x</sub>-pPFBMA<sub>y</sub> particles were treated with thiols in order to study their reactivity in *para*-fluoro substitution reactions and morphological consequences of the modification, see Scheme 1.



**Scheme 1.** Synthesis of pPEGMA<sub>x</sub>-pPFBMA<sub>y</sub> diblock copolymer nano-objects and post-polymerization modification with thiols

## 2.1 Synthesis of pPEGMA<sub>x</sub>-pPFBMA<sub>y</sub>

Five pPEGMA macro-CTAs with degrees of polymerization ranging from 15 to 30 (calculated from conversions) and dispersities between 1.16 and 1.21 (measured by size exclusion chromatography (SEC)) were used, see Supporting Information for synthetic details. Chain extensions of pPEGMA with PFBMA were carried out in ethanol at 70 °C overnight at varying targeted degrees of polymerization ( $y = 43\text{--}203$ ) and aiming at final particle concentrations of 20 wt-%. Copolymerizations reached near-quantitative monomer conversion ( $> 97\%$ ) as determined by  $^1\text{H}$  NMR spectroscopy. In total, 32 formulations were conducted with all

experiments resulting in chain extension and PISA. Expectedly, measured (SEC) and calculated ( $^1\text{H}$  NMR spectroscopy) molecular weights increased with increasing targeted degrees of polymerization of the core-forming block. SEC-measured dispersities,  $\mathcal{D}$ , ranged between 1.33 and 1.58, somewhat higher than expected for RAFT polymerization, which was attributed to possible cross-linker impurities in the commercial PEGMA monomer. Similarly high dispersities have been reported for PISA formulations using pPEGMA as the stabilising block.<sup>[20-22]</sup> A summary of all nanoparticles with compositions, SEC data, and hydrodynamic diameters (measured by dynamic light scattering) is given in Table S3.

## 2.2 Morphologies of pPEGMA<sub>x</sub>-pPFBMA<sub>y</sub>

Self-assembled nanoparticles were analysed by recording bright field images through scanning transmission electron microscopy (STEM). Observed morphologies are given in Table S3 and are plotted in a phase diagram (Figure 1A). For the longer stabilising blocks, pPEGMA<sub>28</sub> and pPEGMA<sub>30</sub>, only spherical particles were found with pPFBMA degrees of polymerization,  $y \leq 203$ , while PISA formulations based on the shorter pPEGMA<sub>15</sub> and pPEGMA<sub>16</sub> stabilising blocks exhibited the full range of morphologies. For several formulations, mixed phases were observed which was attributed to the high dispersities of the diblock copolymers. The relatively high glass transition temperature,  $T_g = 65\text{ }^\circ\text{C}$ <sup>[17]</sup> of the pPFBMA block was considered to facilitate kinetically frozen spherical particles.<sup>[4, 23, 24]</sup> Representative STEM images of pure spherical (S), worm-like (W) and vesicular (V) morphologies are shown in Figure 1B.

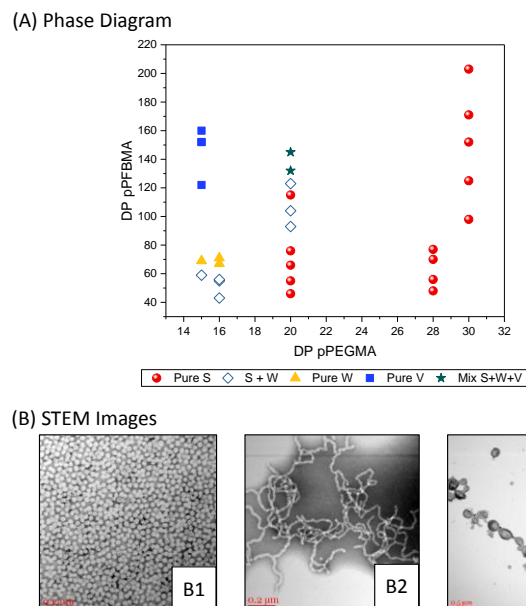


**Figure 1.** (A) Phase diagram showing the observed morphologies of pPEGMA<sub>x</sub>-pPFBMA<sub>y</sub> particles with the degrees of polymerization of the stabilising and core-forming blocks plotted on the x- and y-axis, respectively. (B) Representative STEM images of spherical (S) (pPEGMA<sub>28</sub>-pPFBMA<sub>77</sub>, **B1**), worm-like (W) (pPEGMA<sub>16</sub>-pPFBMA<sub>67</sub>, **B2**) and vesicular (V) (pPEGMA<sub>15</sub>-pPFBMA<sub>160</sub>, **B3**) morphologies.

### 2.3 Temperature responsiveness

Syntheses resulted in liquid dispersions for all samples made with pPEGMA<sub>20</sub>, pPEGMA<sub>28</sub> and pPEGMA<sub>30</sub>, while those made with pPEGMA<sub>15</sub> and pPEGMA<sub>16</sub> presented as gels or consisted of gel and liquid. Gels showed reversible degelation upon heating. STEM images were recorded of samples prepared at different temperatures and indicated that the degelation was based on a transition from worms (25 °C, where physical entanglement is believed to cause gelation) to spheres (60 °C, forming a free-flowing solution), see Figure 2A for representative STEM images and optical photographs. This thermoreversible order–order transition is well documented for alcoholic PISA formulations.<sup>[3, 4, 7]</sup> Overall, PFBMA enabled the preparation of polymorphic nanoparticles via PISA, including thermoresponsiveness, comparable to non-

fluorinated monomers such as benzyl methacrylate. Interestingly, pPEGMA<sub>15</sub>-pPFBMA<sub>69</sub> particles were found to present as worms at 5 °C and formed spheres and vesicles at 60 °C, see Figure 2B. This unexpected phase transition was observed independent of whether the sample was first heated (at its native concentration of 20 wt-%) and then diluted (to 1 g/L for STEM sample preparation), or first diluted (to 1 g/L) and then heated.

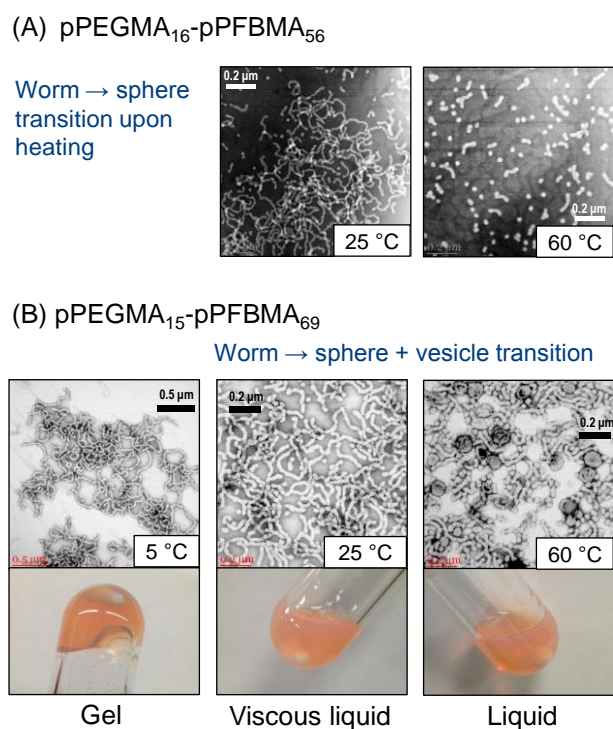


**Figure 2** (A) STEM images of pPEGMA<sub>16</sub>-pPFBMA<sub>56</sub> nano-objects at 25 °C (presenting as worms) and at 60 °C (mostly spheres). (B) STEM images and associated digital photographs of pPEGMA<sub>15</sub>-pPFBMA<sub>69</sub> at 5 °C (worms), 25 °C (mostly worms and some spheres) and 60 °C (mostly spheres, short worms, and—unexpectedly—vesicles)



## 2.4 Post-polymerization modification

With a series of novel nanoparticles in hand, the reactivity of their pPFBMA cores toward thiol-*para*-fluoro substitution was investigated next. This chemistry proceeds quickly and quantitatively in aprotic solvents such as DMF in the presence of strong bases able to deprotonate thiols<sup>[17, 25]</sup> but is less efficient in protic solvents (including ethanol)<sup>[8]</sup> in which the formation of thiolates can be hampered by solvent acidity.

Post-polymerization modifications were first carried out on nano-spheres to optimise the reaction conditions. Spherical pPEGMA<sub>28</sub>-pPFBMA<sub>77</sub> particles (1 equiv of PFB groups) were reacted with 1-octanethiol and 1-butanethiol using 1,8-diazabicyclo[5.4.0]undec-7-ene (DBU) as base (1 equiv each) at 40 °C. After 7 h, <sup>19</sup>F NMR spectroscopic analysis showed that the signal of the *meta*-fluorine atoms had shifted from -161.7 ppm (unmodified) to -134.1 ppm, in agreement with the literature.<sup>[17]</sup> The shifted signal of the replaced fluorine ( $\delta = -122$  ppm) disappeared after purification by dialysis. However, conversions (calculated from <sup>19</sup>F NMR integration) were found to be low at 52% (1-octanethiol) and 49% (1-butanethiol). Reactions were thus let to proceed longer, but, after 10 h, precipitation was observed. It was theorised that the presence of the strong base enabled ethanol (as ethanolate) to transesterify methacrylate units. Indeed, <sup>1</sup>H NMR spectroscopy (not shown) indicated minor amounts (< 5 mol-%) of ethyl methacrylate repeat units in reactions that were left to react for 10 h. The presence of these groups was believed to influence polymer polarity and cause the observed precipitation by decreasing the solubility of the stabilizing block. Instead, thiol-*para*-fluoro reactions were tested at 60 °C for 1 h using an excess (1.5 equiv) of thiols and DBU. Thus, pPEGMA<sub>15</sub>-pPFBMA<sub>59</sub> spherical particles were modified with 1-octanethiol and benzyl mercaptan. Precipitation was not observed for these cases and conversions calculated from <sup>19</sup>F NMR spectroscopy were 64% (1-octanethiol) and 94% (benzyl mercaptan), demonstrating near quantitative conversion for the latter case, see Figure 3. Particle precipitation was observed if

reactions were allowed to react for 2 h or longer at 60 °C. The higher reactivity of benzyl mercaptan compared to 1-octanethiol was attributed to their different acidities ( $pK_{a,1\text{-octanethiol}} = 10.64$ ,<sup>[26]</sup>  $pK_{a,\text{benzyl mercaptan}} = 9.43$ <sup>[27]</sup> in water at 25 °C), suggesting that benzyl mercaptan is more ionised and thus more nucleophilic than 1-octanethiol under similar conditions.

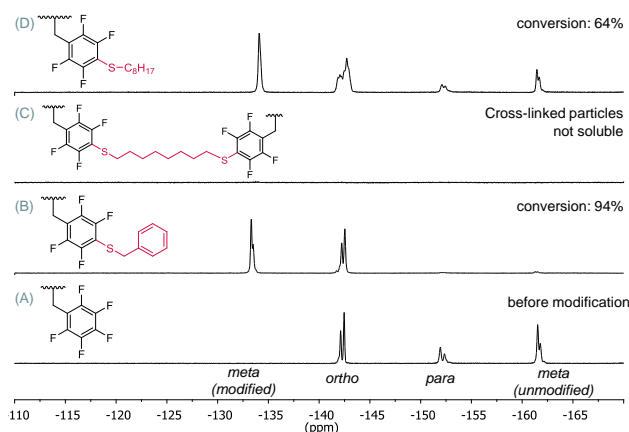


**Figure 3.**  $^{19}\text{F}$  NMR spectra (376 MHz,  $\text{CDCl}_3$ ) of  $\text{pPEGMA}_{15}\text{-pPFBMA}_{59}$  before (A) and after *para*-fluoro substitution with benzyl mercaptan (B), 1,8-octanedithiol (C), and 1-octanethiol (D) at 60 °C for 1 hour in ethanol. Signals showed splitting due to backbone tacticity in agreement with the literature.<sup>[17]</sup>

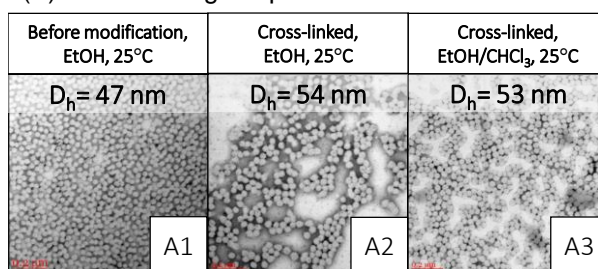
## 2.5 Cross-linking

With reactions indicating that the core-forming blocks of  $\text{pPEGMA}_x\text{-pPFBMA}_y$  PISA particles could be modified with moderate to high conversions, cross-linking reactions were explored next. Cross-linking is essential to prevent particle disintegration in non-selective solvents and may thus widen the applications of well-defined PISA-made nano-objects.

$\text{pPEGMA}_{28}\text{-pPFBMA}_{77}$  spheres were treated with 1,8-octanedithiol in the presence of DBU. 0.8 equiv of dithiol (corresponding to 1.6 thiols per PFB units) were employed.  $^{19}\text{F}$  NMR analysis of a sample in  $\text{CDCl}_3$  did not show any peaks (Figure 3C), precluding an estimation

of the conversion, but suggesting that particles were not dissociating and NMR signals were broadened to the extent of not being visible. In order to demonstrate successful cross-linking, dynamic light scattering (DLS) measurements and STEM imaging were performed before and after thiol-*para*-fluoro modification in ethanol and in an ethanol-chloroform 50:50 by volume. Before modification, the observed sizes in ethanol (hydrodynamic diameter,  $D_h = 47$  nm) and in ethanol-chloroform ( $D_h < 5$  nm) showed that unmodified nano-spheres dissolved unimerically in the solvent mixture (the solubility of a pPFBMA<sub>70</sub> homopolymer<sup>[17]</sup> in ethanol-chloroform (50:50 by volume) was also experimentally confirmed). After modification, the particle diameter in ethanol ( $D_h = 54$  nm), and in ethanol-chloroform ( $D_h = 53$  nm) were similar, demonstrating that particles had increased in size through cross-linking and did not disintegrate in the solvent mixture. DLS-measured size dispersities (Figure S1) of particles before cross-linking (ethanol) and after (ethanol and ethanol-chloroform) were also similar, suggesting that the *para*-fluoro substitution reaction did not adversely affect particle integrity. These observations are supported by STEM images, Figure 4A.

(A) Cross-linking of spheres



(B) Cross-linking of worms

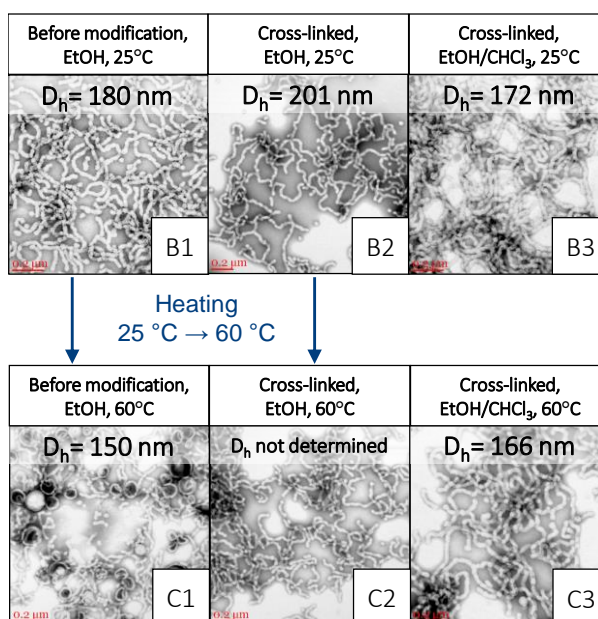


**Figure 4.** 1,8-Octanedithiol cross-linking of nano-spheres and nano-worms: STEM images and average (sphere-equivalent) particle diameters measured by DLS of (A) pPEGMA<sub>28</sub>-pPFBMA<sub>77</sub> nano-spheres; (B) pPEGMA<sub>15</sub>-pPFBMA<sub>69</sub> nano-worms; and (C) pPEGMA<sub>15</sub>-pPFBMA<sub>69</sub> nano-worm samples heated to 60 °C showing thermoresponsiveness only before cross-linking. Polymer concentrations were 1 g/L in ethanol and 0.5 g/L in ethanol–chloroform.

Finally, the cross-linking of temperature-responsive worm-shaped particles was investigated. A sample of pPEGMA<sub>15</sub>-pPFBMA<sub>69</sub> was treated with 1,8-octanedithiol (1.5 equiv) and DBU (1.5 equiv) at room temperature for 7 h. This temperature was chosen as this sample underwent a morphological transition to spheres and vesicles upon heating (Figure 2B). Again, the reaction efficiency could not be determined by <sup>19</sup>F NMR spectroscopy, suggesting that the nanoparticles did not dissolve in CDCl<sub>3</sub>. STEM analysis after cross-linking revealed worm-shaped particles in ethanolic solution and in ethanol–chloroform, indicating that the *para*-fluoro substitution had not influenced the morphology but had led to successful cross-linking. DLS-measured average hydrodynamic diameters increased from  $D_h = 180$  nm before cross-linking to  $D_h = 201$  nm after cross-linking, showing a similar trend as spherical particles (Figure 4A). In the non-selective ethanol–chloroform solvent mixture,  $D_h = 172$  nm was measured. While this lower diameter could be interpreted to be a result of partial nano-worm disintegration due to incomplete cross-linking, it is worth noting that DLS assumes a spherical particle shape and that plasticization of the core-forming block by the non-selective solvent may lead to lower nano-worm rigidity and lower apparent hydrodynamic diameters at unchanged contour lengths. Unlike the uncross-linked sample, the 1,8-octanedithiol-treated nano-worms did not undergo a morphological transition upon heating to 60 °C, with STEM samples prepared in ethanol and in ethanol–chloroform at 60 °C showing worms, while DLS indicated similar hydrodynamic diameters of the cross-linked worms in ethanol–chloroform at 25 °C ( $D_h = 172$  nm) and at 60 °C ( $D_h = 166$  nm), Figure 4C.

### 3. Conclusion

A novel ethanolic PISA formulation was developed using pentafluorobenzyl methacrylate as the core-forming species. It allows the preparation of well-defined nano-objects of spherical, worm-like, and vesicular morphology including temperature-responsive nanoparticle dispersions that undergo reversible morphological transitions. At the same time, the core-forming block is reactive and can be modified in up to near quantitative conversions with thiols in the presence of base. This chemistry was exploited to cross-link nano-spheres and nano-worms, which prevented their disintegration in non-selective solvents. Additionally, cross-linked nano-worms were no longer temperature responsive and did not undergo a morphological transition upon heating. While reversible degelation of PISA-made particles is promising for several applications,<sup>[5]</sup> the narrow thermal and compositional window in which worm-shaped particles are found can be a nuisance, and temperature changes or chemical modification of the solubilising block can result in an unintended loss of the gel-forming worm morphology. PISA and subsequent core-cross-linking of PFBMA presents an efficient method to retain particle morphology across a temperature range and in non-selective solvents without changes to the solubilising block. *Para*-fluoro substitution chemistry on the cores of PISA-made particles further holds potential to influence the morphology of a precursor, which we are currently exploring.

**Key Words.** Thiol-*para*-fluoro reaction, nanoparticle cross-linking, temperature-responsiveness, PISA, postpolymerization modification

**Supporting Information.** Supporting Information is available from the Wiley Online Library or from the Author.

**Acknowledgement.** The authors acknowledge the University of Surrey for an NPL-Surrey studentship for N.B.

## References

- [1] A. Blanz, S. P. Armes, A. J. Ryan, *Macromol Rapid Commun* **2009**, *30*, 267.
- [2] J. Rieger, *Macromolecular Rapid Communications* **2015**, *36*, 1458.
- [3] M. J. Derry, L. A. Fielding, S. P. Armes, *Progress in Polymer Science* **2016**, *52*, 1.
- [4] A. B. Lowe, *Polymer* **2016**, *106*, 161.
- [5] N. J. Warren, S. P. Armes, *Journal of the American Chemical Society* **2014**, *136*, 10174.
- [6] B. Charleux, G. Delaittre, J. Rieger, F. D'Agosto, *Macromolecules* **2012**, *45*, 6753.
- [7] Y. Pei, A. B. Lowe, P. J. Roth, *Macromolecular Rapid Communications* **2017**, *38*, 1600528.
- [8] Y. Pei, J.-M. Noy, P. J. Roth, A. B. Lowe, *Polymer Chemistry* **2015**, *6*, 1928.
- [9] Y. Pei, J.-M. Noy, P. J. Roth, A. B. Lowe, *Journal of Polymer Science Part A: Polymer Chemistry* **2015**, *53*, 2326.
- [10] Y. Pei, A. B. Lowe, *Polym. Chem.* **2014**, *5*, 2342.
- [11] R. Deng, M. J. Derry, C. J. Mable, Y. Ning, S. P. Armes, *Journal of the American Chemical Society* **2017**, *139*, 7616.
- [12] L. P. D. Ratcliffe, C. Couchon, S. P. Armes, J. M. J. Paulusse, *Biomacromolecules* **2016**, *17*, 2277.
- [13] S. J. Byard, M. Williams, B. E. McKenzie, A. Blanz, S. P. Armes, *Macromolecules* **2017**, *50*, 1482.
- [14] W. Zhou, Q. Qu, W. Yu, Z. An, *ACS Macro Letters* **2014**, *3*, 1220.
- [15] J. Huang, H. Zhu, H. Liang, J. Lu, *Polymer Chemistry* **2016**, *7*, 4761.
- [16] J. R. Lovett, L. P. Ratcliffe, N. J. Warren, S. P. Armes, M. J. Smallridge, R. B. Cracknell, B. R. Saunders, *Macromolecules* **2016**, *49*, 2928.
- [17] J.-M. Noy, A.-K. Friedrich, K. Batten, M. N. Bhebhe, N. Busatto, R. R. Batchelor, A. Kristanti, Y. Pei, P. J. Roth, *Macromolecules* **2017**, *50*, 7028.

- [18] S. Agar, E. Baysak, G. Hizal, U. Tunca, H. Durmaz, *Journal of Polymer Science Part A: Polymer Chemistry* **2018**.
- [19] G. Delaittre, L. Barner, *Polymer Chemistry* **2018**.
- [20] Y. Pei, K. Jarrett, M. Saunders, P. J. Roth, C. E. Buckley, A. B. Lowe, *Polymer Chemistry* **2016**, 7, 2740.
- [21] J. Yeow, O. R. Sugita, C. Boyer, *ACS Macro Letters* **2016**, 5, 558.
- [22] G. Wang, M. Schmitt, Z. Wang, B. Lee, X. Pan, L. Fu, J. Yan, S. Li, G. Xie, M. R. Bockstaller, K. Matyjaszewski, *Macromolecules* **2016**, 49, 8605.
- [23] J. van Stam, S. Creutz, F. C. De Schryver, R. Jérôme, *Macromolecules* **2000**, 33, 6388.
- [24] Y. Pei, N. C. Dharsana, J. A. van Hensbergen, R. P. Burford, P. J. Roth, A. B. Lowe, *Soft Matter* **2014**, 10, 5787.
- [25] J.-M. Noy, M. Koldevitz, P. J. Roth, *Polymer Chemistry* **2015**, 6, 436.
- [26] M. Moreno, G. Lligadas, J. C. Ronda, M. Galià, V. Cádiz, *Green Chem.* **2014**, 16, 1847.
- [27] M. M. Kreevoy, E. T. Harper, R. E. Duvall, H. S. Wilgus, L. T. Ditsch, *Journal of the American Chemical Society* **1960**, 82, 4899.



## For Table of Contents Use Only

Polymer nanoparticles with tuneable morphologies, temperature-responsiveness, and reactive cores were prepared through RAFT dispersion polymerization and polymerization-induced self-assembly (PISA) based on 2,3,4,5,6-pentafluorobenzyl methacrylate. *Para*-fluoro substitution with a dithiol successfully crosslinked nanoparticles resulting in temperature-independent morphology retention in non-selective solvents.

